



ELSEVIER

Available online at www.sciencedirect.com



Fluid Dynamics Research III (III) III-III

FLUID DYNAMICS
RESEARCH

1

Vortex collapse and turbulence

3

R.M. Kerr*

Centre for Scientific Computing, University of Warwick, Coventry CV4 7AL, UK

5

Received 16 September 2003; received in revised form 31 July 2004; accepted 14 September 2004

Communicated by S. Kida

7

Abstract

Recent calculations related to the self-induced collapse of large-scale vortex structures into fine scale, possibly singular, structures in the Euler and Navier–Stokes equations are described. The practical importance of these intense events is their possible role in turbulence through the effects of strong intermittency and how that will direct turbulence modelling. Despite a concerted international effort to simulate these events over a decade ago, their dynamical origin remains largely unknown. A new international collaboration designed to push our understanding of the Euler singularity problem is described. These events are closely related to one of the outstanding mathematical questions of our time: whether solutions of the three-dimensional incompressible Navier–Stokes equations, lying in a bounded domain with finite energy and no external forcing, remain regular for arbitrarily long times (www.claymath.org/Millennium_Prize_Problems).

© 2005 Published by The Japan Society of Fluid Mechanics and Elsevier B.V. All rights reserved.

Keywords: Turbulence; Vortex dynamics; Direct numerical simulation

19

1. Introduction

While the dynamics of isolated vortex sheets and tubes in turbulent flow can be described by simple models such as a stretched Burgers vortex, the interactions between vortex structures are not well understood. The objectives of this contribution are to summarize our current knowledge of intense three-dimensional vortex interactions in numerical simulations, discuss new plans for investigating these issues, and to review a new result for how vortex tubes might form from generic initial conditions.

* Tel.: +44 24 765 74415; fax: +44 24 765 24182.

E-mail address: Robert.Kerr@warwick.ac.uk

1 The underlying mathematical problem is that the Navier–Stokes equations are smooth in space, while
2 turbulence generated by them is an ensemble of vortex structures that are smooth only on the smallest
3 scales, and possibly not even there. Both experimentally and numerically we know that vortex tubes can
4 persist a relatively long time when in isolation. In contrast, vortex sheets are transient structures found
5 within shear layers or when interacting vortex tubes tear each other apart. Whether or not these structures
6 are smooth at the smallest scales is the “regularity” problem in the Navier–Stokes equations. That is,
7 could singularities be generated by the Navier–Stokes equations in a finite time from smooth, finite-
8 energy initial conditions? The folklore is that they are regular, but at present there is nothing we know
9 from the mathematics or the properties of its inviscid form, the Euler equations, to rule out singularities
10 in the Navier–Stokes equations.

11 If the Euler equations were regular, then it should automatically follow that the Navier–Stokes equations
12 are also regular because viscosity provides an additional smoothing term (Constantin, 1986). For many
13 years it was thought that the Euler equations would be regular because numerical solutions showed
14 suppression of the nonlinear terms. However, roughly 10 years ago several calculations showed properties
15 consistent with the generation of singularities in the Euler equations. These suggestive results need to be
16 considered in much greater detail if the results are to be proven robust. We also need to consider whether
17 the initial conditions leading to possible singularities are the proper initial conditions for a turbulent
18 flow.

19 This contribution will be organized as follows. First, an international collaboration that will look
20 at the singularity questions anew will be described. Then older mathematical and computational re-
21 sults are reviewed. Finally, new three-dimensional graphics are presented for one smooth initial con-
22 dition that demonstrates a newly identified transverse configuration for interacting vortex structures in
23 Navier–Stokes. In the summary, questions raised by these results concerning the route a fluid will take in
24 going from smooth initial conditions to $-\frac{5}{3}$ Navier–Stokes turbulence are discussed.

25 2. International collaboration

26 The first serious numerical attempt to determine whether singularities might form in either the three-
27 dimensional Euler or Navier–Stokes equations used the Taylor–Green initial condition (Brachet et al.,
28 1983). This initial condition consists of just a few Fourier modes with strong symmetries. The first
29 structures to form were vortex sheets and eventually vortex tubes appeared. Using the spectral tests
30 available in 1983, up to the last time that the Euler equations could be run there was no evidence of
31 singular behavior.

32 An effective analytical test was not proposed until 1984, when it was shown that the time integral of
33 the peak vorticity $\int \omega_p dt$ had to become singular for any possible singularity of the Euler equations to
34 form (Beale et al., 1984). This is important for numerics because only first derivatives of the velocity
35 field need to be calculated. It was not until the mid-1990s that numerical simulations began to show
36 vorticity growth consistent with the time integral test. The cases were antiparallel vortices (Kerr, 1993), a
37 sheared cylindrical vortex (Grauer et al., 1998) and inviscid orthogonal vortices (Brandenburg and Kerr,
38 2001). The strongest growth in the peak vorticity and most detailed numerical analysis was for antiparallel
39 vortices. For the other two cases, indications are that at the smallest scale they are also collapsing into the
40 antiparallel configuration. Through different tests it has also been suggested that the Kida vortex could
41 become singular (Boratav and Pelz, 1997).

1 All of these calculations are at least 5 years old. In the intervening period, computational resources
 3 have grown and numerical methods for refining in localized regions have improved. Therefore, we believe
 5 that the time is ripe to revisit many of the vortex collapse problems. A developing collaboration among
 7 Imperial College, Warwick University, the Nice Observatory, Rutgers University, the University of New
 Hampshire and Kyoto University has been proposed for revisiting the vortex collapse problems at high
 numerical resolution. Plans for this collaboration were originally to be discussed with R. Pelz. After his
 tragic death, a new planning meeting was arranged at the Institute for Advanced Study.

The plan is to attack initial conditions considered before, plus a few new ones, with at least two numerical
 methods. The collaboration would include researchers familiar with traditional spectral methods, adaptive
 mesh finite difference methods, and spectral element methods.

11 3. Background

13 3.1. Mathematical history

The most significant mathematical advance in this field is the result by Beale et al. (1984) proving that
 all possible singularities of the Euler equations are controlled by the time integral of the maximum of the
 vorticity (designated $\|\omega\|_\infty$). That is, there can be a singularity at $t = T$ only if

$$\int_0^t \|\omega\|_\infty d\tau \rightarrow \infty \quad \text{as } t \rightarrow T.$$

The simplicity of this result provided the community with a method for excluding results due to numerical
 artifacts and thereby encouraged a serious search for singularities of the Euler equations in numerical
 calculations.

Fig. 1 gives an overview of the physical meaning of this result. If there are two neighboring vortex
 regions (far left), a singularity can form only if their surfaces are pushed together (far right). If the
 separation of their surfaces goes as δ , e is the strain pushing them together, and assuming that

$$\frac{d\delta}{dt} = -e\delta$$

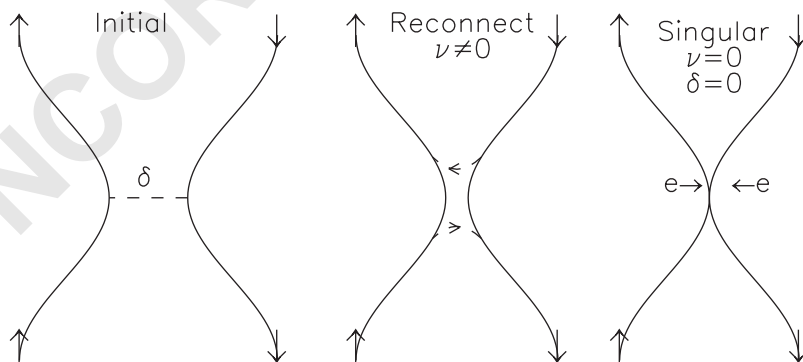


Fig. 1. Diagram of the interaction of antiparallel vortices. From an initial condition of antiparallel vortices separated at their
 closest approach by δ , if $\nu \neq 0$ there is reconnection that forms new vortices indicated by the dashed curves. However, if $\nu = 0$,
 a singularity can form if $\delta = 0$ at a point as the vortices are pushed together by the self-induced strain indicated by e .

1 then in order for $\delta \rightarrow 0$, one must have

$$\int e \, dt \rightarrow \infty,$$

3 which is mathematically equivalent to stating that $\int_0^t \|\omega\|_\infty \, d\tau \rightarrow \infty$.

5 There are now three related two-dimensional systems whose singular behavior, or lack thereof, is largely understood. These are two-dimensional turbulence, a quasigeostrophic (2D QG) model, and stretched Euler. The two-dimensional Euler equations do not have vortex stretching and are therefore regular. For a 2D QG model there is a result similar to [Beale et al. \(1984\)](#), from which new tests were found based upon bounds on the curvature of active lines and the velocity ([Constantin et al., 1994](#)). Presently, a similar proof for three-dimensional Euler equations requires one additional assumption ([Constantin et al., 1996](#)).

11 The stretched Euler model is a “two and one-half dimensional” Euler system whose velocity field takes the form reminiscent of the Burgers vortex $\{u_1(x, y, t), u_2(x, y, t), z\gamma(x, y, t)\}$, with the u_3 component is linear in z ([Ohkitani and Gibbon, 2000](#)). Although this is an infinite energy system and is not directly relevant to the singularity question for Euler posed above, this system allows us to test our numerical analysis tools.

15 Refined numerical tests have suggested that the 2D QG model is not singular ([Ohkitani and Yamada, 1997](#)), but the 2D stretched Euler model might be ([Ohkitani and Gibbon, 2000](#)). It is now known analytically that these results are correct ([Cordoba and Fefferman, 2001, 2002; Constantin, 2000](#)). These results demonstrate two aspects of how we plan to approach the three-dimensional Euler problem. First, there are numerical tests similar to those planned in three dimensions that have successfully predicted the analytical behavior in two dimensions. Second, that close interaction between those working and thinking about the numerical and analytic problems is necessary to make progress.

3.2. First evidence for singularities

23 Before 1993, calculations of the Euler equations generally showed depletion of the nonlinearity and suppression of trends towards singularities. The depletion of nonlinearity was tied to the appearance of vortex sheets, which introduces a degree of two dimensionality or lack of three-dimensional curvature. Because the two-dimensional Euler equations are known to be regular, it was believed that these structures would prevent the formation of singular behavior.

29 The important change in the numerics that led to more singular behavior was how smooth initial conditions were set. For truly smooth large-scale initial conditions, such as the Taylor–Green vortex or a small set of low-wavenumber random Fourier modes, this is not a problem. But in those cases, the first strong dynamics is the formation and rapid thinning of vortex sheets. Eventually a configuration that might be disposed to becoming singular appears, but by this time the structures are at the resolution of the largest uniform mesh calculations feasible and further inviscid development cannot be followed.

35 The strategy for following possible singular development further is to begin with well-defined, compact vortices that are taken from the calculations with smooth large-scale initial conditions and from vortex filament calculations suggesting singular behavior ([Chorin, 1982; Pumir and Siggia, 1987](#)). If these well-defined vortices are on the largest scales of the calculation, then hopefully by the time they have generated small scales of the order of the mesh size, some evidence of singular behavior will appear. However, to go from truly smooth initial conditions to initial conditions that might have a jump in vorticity at a boundary could induce unphysical effects. For example, all evidence points to a cusp singularity in

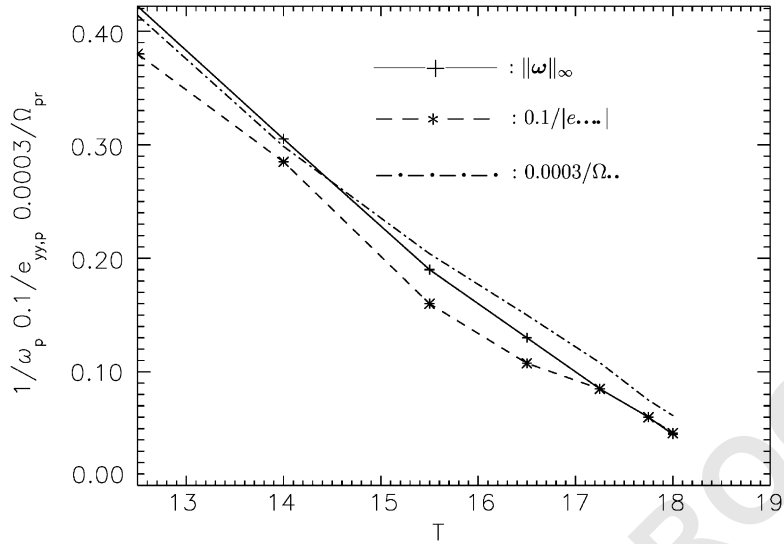


Fig. 2. Dependence of $1/\|\omega\|_\infty$, $0.1/|e_{yy,p}|$ and $0.0003/\Omega_{pr}$ upon time from the antiparallel Euler calculation showing convergence to a singular time of about $T = 18.7$.

- 1 the rollup of an infinitesimally thin vortex sheet of finite strength. This might appear to violate the known
 2 regularity of two-dimensional Euler, but it does not because the initial condition is itself initially singular.
 3 If the two-dimensional vortex sheet has any thickness, there will be no singularities as it rolls up.
 4 Therefore, the compact vortex initial condition must initially be as smooth as the final state found from
 5 the large-scale smooth initial conditions. To achieve this, one can take any nearly smooth profile for the
 6 initial vortices and apply a hyperviscous filter (Kerr and Hussain, 1989). The best initial condition for
 7 antiparallel vortices (Kerr, 1993) was obtained by combining a profile all of whose derivatives are smooth
 8 at a given radius with a hyper-viscous filter, as detailed elsewhere (Kerr, 1992). The strategy chosen by
 9 Boratav et al. (1992) for orthogonal vortices was to apply a hyperviscosity on every time-step. Note that
 10 in order to develop a complete picture at least two types of simulations are needed: those with initially
 11 smooth large scales to get an overview of the possible types of structures and those with compact vortices
 12 as the initial condition to understand the details of the small scales that develop.

13 3.3. Compact vortex initial conditions

- 14 Evidence for singularities and the structures that develop for initially antiparallel and orthogonal vor-
 15 tices will now be given. All of these calculations have used periodic boundary conditions. The best
 16 orthogonal calculations have used only uniform meshes and symmetries in the antiparallel initial condi-
 17 tion allow some adaptivity to be applied. Using a filtered antiparallel initial condition, Kerr (1993) was
 18 able to generate growth in $\|\omega\|_\infty$ by a factor of 24 and growth of two independent possibly singular
 19 quantities by a factor of 8. Fig. 2 shows that all three quantities,

$$\omega_p = \|\omega\|_\infty, \quad |e_{yy,p}|, \quad \text{and} \quad \Omega_{pr} = \int dV \omega_i e_{ij} \omega_j \quad (1)$$

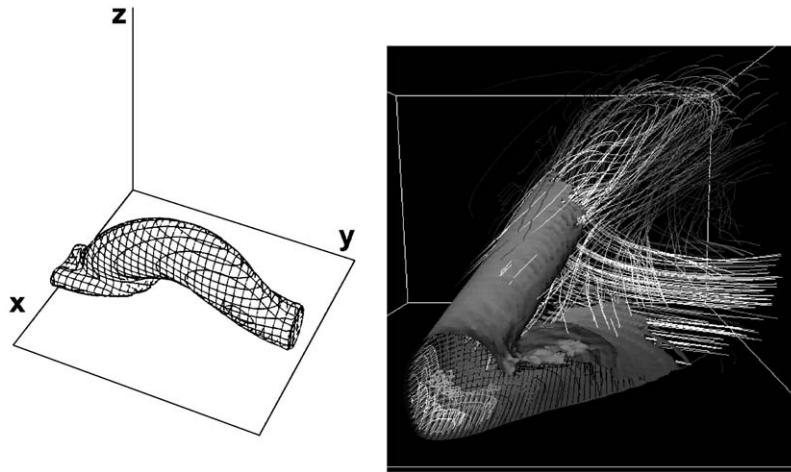


Fig. 3. Two views of one-half of one of the interacting antiparallel vortices. The left frame, from Kerr and Hussain (1989) is an isosurface of vorticity in the original coordinate frame. The right frame, from Kerr (1996) is a blowup of the flattened region with the dimple, with the z -direction amplified by an additional factor of five. Shown are an isosurface of vorticity, shaded contours of $|\omega|$ in the symmetry plane, and vortex lines that originated in the vicinity of ω . In each frame $\frac{1}{2}$ of one of the two vortices is shown. Imagine that the vortex continues with a mirror symmetry through the x - z plane and there is a mirror image of this full vortex across the x - y plane. Maximum vorticity is by symmetries in the x - z plane. The shaded contours through that plane in the right frame show that the position of $\|\omega\|_\infty$ is in the lower left corner of this structure.

1 blow up as $(T - t)^{-1}$, where $T = 18.7$ is their common projected singular time. Therefore, consistency
 2 with the constraints of Beale et al. (1984) is shown. The subscript yy, p indicates this is the peak value of
 3 the strain eigenvalue along the direction of vorticity at the position of the peak vorticity in the symmetry
 plane. Two values of the axial strain e_{yy} in the symmetry plane ($y = 0$) were tracked:

5 $e_{yy,p}$ the peak value of e_{yy} and $e_{yy,m}$ the value of e_{yy} at $\|\omega\|_\infty$.

The ratio $\|\omega\|_\infty/|e_{yy,m}| \approx 19$.

7 Fig. 3 presents two views of one-half of one of the interacting antiparallel vortices. Note the flattening
 8 of the original vortex tube near the x - z plane in the left frame. This flattening into a vortex sheet is what
 9 earlier calculations had found to be dominant. However, note the dimple in the middle of the sheet, hinting
 at three dimensionality.

11 The right frame is a blowup of the flattened region with the dimple. The sheet-like structure persists
 12 to the lower right, while the dimple becomes the strong bending of this sheet in the left corner. Note also
 13 the vortex lines that leave this inner region and how they are twisting around. Analysis in Kerr (1999)
 14 suggests that the bending of the vortex lines is only moderately strong, their radius of curvature R goes
 15 to zero as $R \sim (T - t)^{1/2}$, while the length scale for the bending of the vortex sheet goes as $\delta \sim (T - t)$.
 It appears that the twisting of vortex lines combined with the bending of the vortex sheet provides the
 17 necessary degree of three dimensionality needed to generate singular behavior.

19 Fig. 4 shows the evolution of inviscid orthogonal vortex tubes. Note the arms pulled out that become
 antiparallel. Once this happens near $t = 6$, $\|\omega\|_\infty$ and $\int dV \omega_i e_{ij} \omega_j$ grow rapidly. Fig. 5 shows two of
 the three properties used for the antiparallel case in Fig. 2. While $|e_{yy,m}|$ (defined above with $|e_{yy,p}|$) is

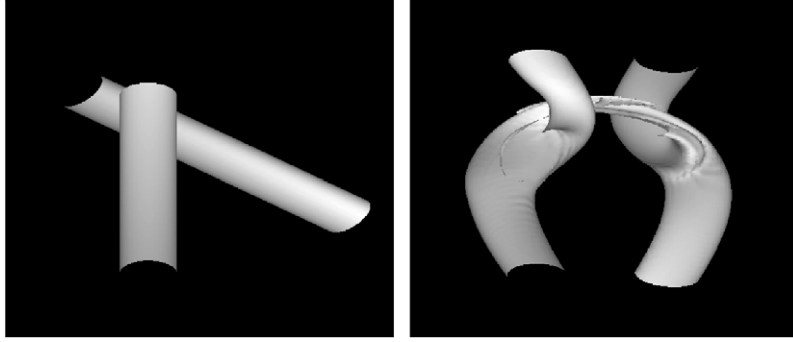


Fig. 4. Orthogonal vortices in Euler. Isosurfaces are a fixed percentage of ω_p in each frame. The two frames are $t = 0$ and 10. Arms are pulled out of the original vortices, become antiparallel, then vorticity within the arms develops singular behavior.

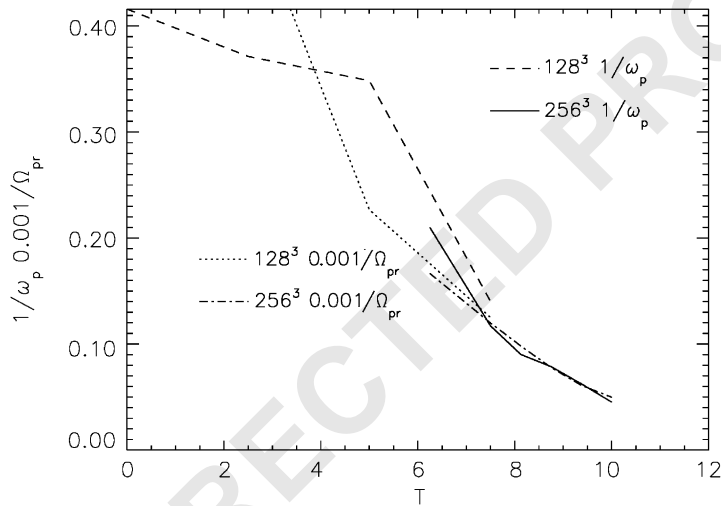


Fig. 5. $1/\|\omega\|_\infty$ and $1/\int \omega_i e_{ij} \omega_j dV$ in Euler for orthogonal vortices.

- 1 difficult to determine directly, the time dependence of $\|\omega\|_\infty$ in Fig. 5 indicates its value. It is found that
 2 the ratio $\|\omega\|_\infty/|e_{yy,m}| = 20 \pm 5$ between $t = 4.5$ and 10, which is consistent with the value of ≈ 19
 3 found in the antiparallel case. The time dependence of $\|\omega\|_\infty$ in the calculations of a cylindrical sheared
 4 vortex (Grauer et al., 1998) also suggests a similar value for the ratio in that case.

5 4. Large-scale smooth initial conditions

4.1. Taylor–Green vortex

- 7 The compact vortex initial conditions were inspired in part by the final state for Euler calculations with
 8 smooth large-scale initial conditions. One might ask how these smooth initial conditions evolve if there
 9 is a small viscosity. Simulations that are smooth on the largest scales suggest that another scenario might
 exist.

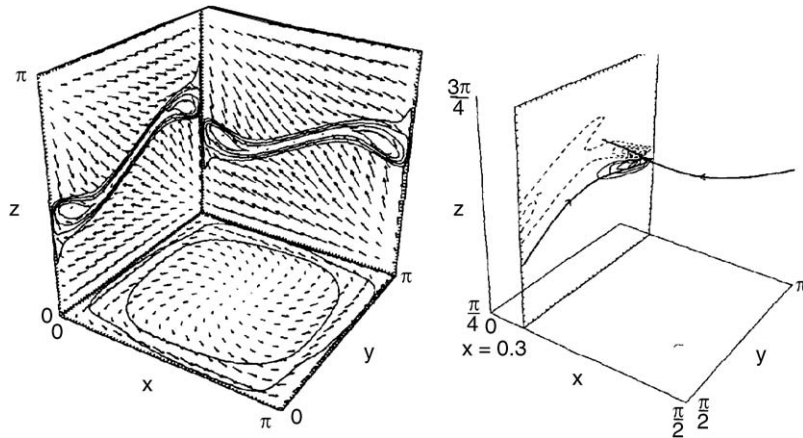


Fig. 6. A nearly inviscid time ($t = 3.5$) for a mildly viscous calculation from Herring et al. (1994). Left frame shows contours of $|\omega|^2$ on symmetry planes and is similar to figures from Brachet et al. (1983), while the right frame shows contours of ω_x from a plane off the symmetry plane as well as vortex lines through the positions of maximum vorticity in the symmetry planes in the left frame.

1 The initial condition for the three-dimensional Taylor–Green vortex is composed of simple combina-
 2 tions of Fourier modes such as $w = \sin(x) \sin(y) \cos(z)$ and was most extensively analyzed by Brachet
 3 et al. (1983). This initial condition is characterized by several symmetries so that only $\frac{1}{4^3}$ of the domain
 4 needs to be simulated. Fig. 6 shows a nearly inviscid time for a mildly viscous calculation using only $\frac{1}{2^3}$
 5 of the possible symmetries. The initial flow is two counter-rotating zones at the top and bottom with a shear
 6 zone between them. The first vortical feature that develops is a sheet within that shear zone. The ends of
 7 that sheet initially develop through interactions with antiparallel neighbors across one of the symmetries.
 8 But this initial development is suppressed as the ends run into another of their images. This is what is
 9 observed along the back edge in the left frame of Fig. 6. Beyond this time (approximately $t = 3.1$ in a
 10 strictly inviscid calculation) either an inviscid calculation must be halted or viscous effects would become
 11 dominant in a Navier–Stokes calculation.

12 Some indication of what might happen next can be found by the three-dimensional extensions of
 13 vorticity in the right frame. It is seen that the vorticity is nearly orthogonal and found in sheets. That
 14 is, the narrow contours through which the vorticity goes in the right frame are an extension of the sheet
 15 structure in the upper right plane of the left frame.

16 By this time the peak vorticity no longer resides in one of the symmetry planes, but is in the plane shown
 17 in the right frame. Does this interaction of orthogonal vorticity in nearly parallel vortex sheets lead to a
 18 singularity? And if so, by what route? Do the lines of most intense vorticity peel off as antiparallel structures
 19 as the cases we have already discussed would suggest? Or is there some other type of nearly singular
 20 interaction? The next case suggests that whatever the answers are to these questions, the orthogonal
 21 vorticity within parallel sheets plays an important role in what develops after reconnection.

4.2. Viscous transverse structures

22 As an example of why a variety of initial conditions need to be studied, and why we should expect to
 23 find new structures, let us consider a smooth initial condition initially proposed for decaying isotropic

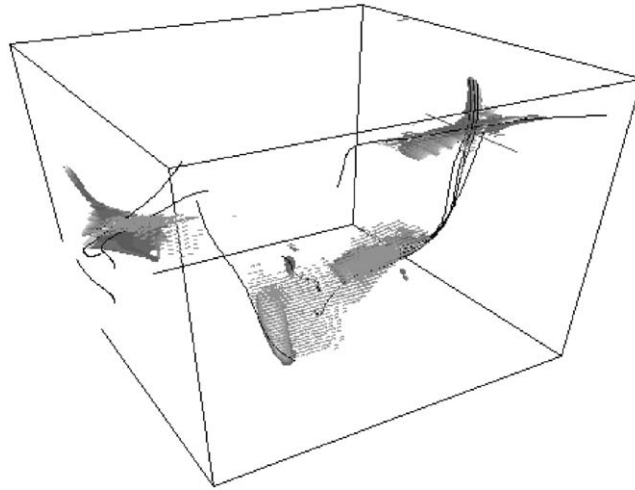


Fig. 7. Isosurfaces of vorticity in flat gray with sample vortex lines through regions given by the threshold for the DNS calculation at $t = 0.5$. Hashes indicate where helicity is large. Helicity is of one sign in the long structure across the domain, and of the opposite sign in the crossing structure in the upper right. $\theta_y = 30$ and the box is such that $\|\omega\|_\infty$ for $t = 0.5$ and 0.7 is contained within it. The location of $\omega_p = \|\omega\|_\infty$ is within the cross in the upper right.

1 turbulence by [Herring and Kerr \(1993\)](#). They noted a timescale of $t = 0.5$ associated with the maximum
 2 value of the peak vorticity. Shortly thereafter, dissipation reaches a maximum, the energy spectrum fills
 3 out to a $-\frac{5}{3}$ power law, and isolated vortex tubes appear. The calculations were Navier–Stokes and the
 4 resolution was never fine enough to expect to see singular trends even if Euler had been run. However,
 5 the maximum of ω_p might point to when vortex reconnection begins.

6 Up until $t = 0.4$ the dominant vortex structures in [Herring and Kerr \(1993\)](#) were vortex sheets. [Holm
 7 and Kerr \(2002\)](#) noted that even though the structures had collapsed at $t = 0.5$, the dominant structures
 8 near ω_p were still sheets. A new coherent mechanism was indicated that was characterized by viscous,
 9 transverse (or orthogonal) vortex sheets gradually transforming themselves into interacting transverse
 10 vortex tubes. The new mechanism does not appear to depend upon either the inviscid rollup of vortex
 11 sheets or the reconnection of antiparallel vortices. The interacting regions in both physical and Fourier
 12 space are characterized by oppositely signed helicity and viscous dissipation plays a role as early at
 13 $t = 0.4$.

14 The final part of this contribution will be additional graphics designed to demonstrate the new dissipation
 15 mechanism. This work is still in progress. [Fig. 7](#) shows the subdomain across which the peak vorticity
 16 moves between $t = 0.5$ and 0.7 . At $t = 0.5$ this subdomain is dominated by a vortex structure that ends
 17 within the transverse vortices in the upper right. The peak vorticity lies within this transverse region
 18 and closer inspection would reveal that the two transverse vortices are nearly sheet-like. The transverse
 19 vortices in the upper right are the same structures that dominate the graphics in [Holm and Kerr \(2002\)](#) at
 20 $t = 0.5$. Color images would show that the helicity in the two structures is of opposite sign. [Fig. 8](#) shows
 21 the evolution along this structure from another angle at a later time $t = 0.7$. The cross bar vortex in the
 22 upper right in [Fig. 7](#) has moved along the dominant vortex, annihilating or reconnecting vorticity and
 23 dissipating energy. By $t = 0.7$ the structures are clearly tubes. [Fig. 9](#) shows the whole box at $t = 0.7$ to

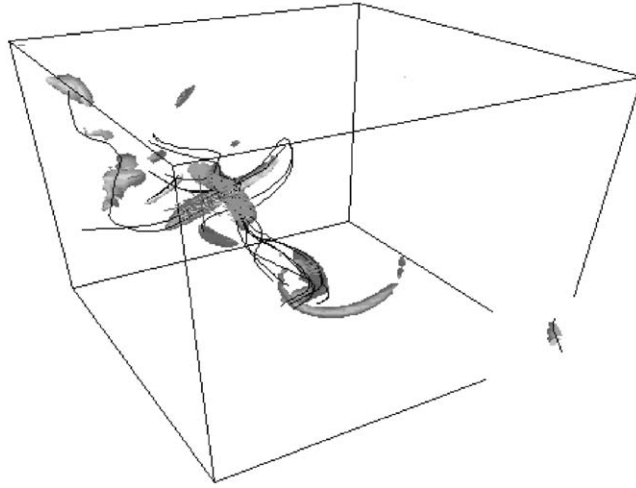


Fig. 8. Isosurfaces and helicity at $t = 0.7$ for the same volume as Fig. 7, but rotated about 90° . The position of $\|\omega\|_\infty$ at $t = 0.5$ had been in the upper left corner and has now dissipated. $\omega_p = \|\omega\|_\infty$ is in the cross in the middle.

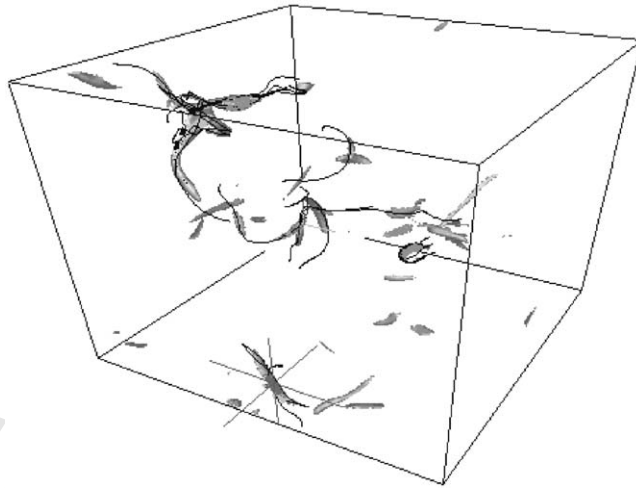


Fig. 9. Isosurfaces and helicity at $t = 0.7$ for the entire simulation. $\omega_p = \|\omega\|_\infty$ is indicated by the cross near the lower boundary, giving a perspective of the size of the boxes in the previous figures.

- 1 demonstrate how small the subdomain of the most intense vorticity is. Note that the structure in Fig. 8
- 3 is now along the lower edge. While it has the most intense vorticity, it is not the largest structure in the domain of Fig. 9. The largest structure is in the upper left and is presumably developing into the next dominant structure.

Table 1

Two scenarios for how vortex tubes form from smooth initial conditions

STAGES

(1) Collision of Blobs	
(2) Appearance of vortex layers (sheets) at $T = 0.25T_e$	
3(A)	3(B)
(a) Enhanced rollup Vortex tubes	(a) Near singularity (But what type?)
Anti-parallel attraction	Orthogonal configuration
(b) $\lim_{v \rightarrow 0} \lim_{T \rightarrow T_c} \ \omega\ _\infty \rightarrow \infty$	(b) Dissipation and reconnection begins. ω is still in layers. Growth of $\ \omega\ _\infty$.
(c) Reconnection:	(c) Dissipation growing
Viscous dissipation	
(d) Isolated tubes	(d) Vortex tubes
(4) Small-scale vortex tube and $E(k) \sim k^{-5/3}$ at $T = T_e$.	

3A is the traditional scenario. 3B is suggested by new numerical results. T_e is an eddy turnover time.

1 5. Conclusion

Given that the Taylor–Green and decaying isotropic simulations started nearly inviscidly, one might ask when the evolution changes from being dominated by inviscid Euler dynamics to viscous Navier–Stokes dynamics. The transition appears during a period of strong vortex alignment, followed by vortex annihilation. How does this transformation conform to previous ideas? And what are the connections between a possible singularity of Euler, vortex reconnection, and the appearance of vortex tubes in Navier–Stokes turbulence?

Table 1 presents two possible scenarios for how vortex tubes might form in an eddy turnover time T_e from smooth initial conditions. The first scenario (3A) assumes that the only type of singularity in the inviscid limit has antiparallel vorticity at the smallest scale. It is assumed that for sufficiently high Reynolds numbers, Navier–Stokes solutions will always develop this configuration at the smallest scales. It would be from this point that vortex reconnection begins and from which dissipation develops. Eventually this should lead to a flow dominated by vortex tubes.

The second scenario (3B) is what might actually have been observed in some of the earlier visualizations of interactions in numerical turbulence, in Taylor–Green (Brachet et al., 1983) and in forced isotropic turbulence (Kerr, 1985). Antiparallel vortex structures are never observed, but helicity clearly plays a major role. It is hoped that the new international collaboration will help resolve these issues.

References

- 19 Beale, J.T., Kato, T., Majda, A., 1984. Remarks on the breakdown of smooth solutions for the 3D Euler equations. *Comm. Math. Phys.* 94, 61.
- 21 Boratav, O.N., Pelz, R.B., 1997. Structures and structure functions in the inertial range of turbulence. *Phys. Fluids A* 9, 1400–1415.
- 23 Boratav, O.N., Pelz, R.B., Zabusky, N.J., 1992. Reconnection in orthogonally interacting vortex tubes: direct numerical simulations and quantification in orthogonally interacting vortices. *Phys. Fluids A* 4, 581–605.
- 25 Brachet, M.E., Meiron, D.I., Orszag, S.A., Nickel, B.G., Morf, R.H., Frisch, U., 1983. Small-scale structure of the Taylor–Green vortex. *J. Fluid Mech.* 130, 411–452.

- 1 Brandenburg, A., Kerr, R.M., 2001. Helicity in hydro and MHD reconnection. In: Barenghi, C.F., Donnelly, R.S., Vinen, J. (Eds.),
Quantized Vortex Dynamics & Superfluid Turbulence. Cambridge University Press, Cambridge.
- 3 Chorin, A., 1982. The evolution of a turbulent vortex. *Comm. Math. Phys.* 83, 517.
- 5 Constantin, P., 1986. Note on loss of regularity for solutions of the 3-D incompressible Euler and related equations. *Comm.*
Math. Phys. 104, 311–326.
- 7 Constantin, P., 2000. The Euler equations and nonlocal conservative Riccati equations. *Int. Math. Res. Notices* 9, 55–65.
- 9 Constantin, P., Majda, A.J., Tabak, E., 1994. Formation of strong fronts in the 2-D quasigeostrophic thermal active scalar.
Nonlinearity 9, 1495–1533.
- 11 Constantin, P., Fefferman, C., Majda, A., 1996. Geometric constraints on potentially singular solutions for the 3D Euler equations.
Comm. Partial Differential Equations 21, 559–571.
- 13 Cordoba, D., Fefferman, C., 2001. Scalars convected by a two-dimensional incompressible flow. *Comm. Pure Appl. Math.* 55,
255–260.
- 15 Cordoba, D., Fefferman, C., 2002. Growth of solutions for QG and 2D Euler equations. *J. Am. Math. Soc.* 15, 665–670.
- 17 Grauer, R., Marliani, C., Germaschewski, K., 1998. Adaptive mesh refinement for singular solutions of the incompressible Euler
equations. *Phys. Rev. Lett.* 80, 4177–4180.
- 19 Herring, J.R., Kerr, R.M., 1993. Development of enstrophy and spectra in numerical turbulence. *Phys. Fluids A* 5, 2792–2798.
- 21 Herring, J.R., Kerr, R.M., Rotunno, R., 1994. Ertel's potential vorticity in unstratified turbulence. *J. Atmos. Sci.* 51, 35.
- 23 Holm, D.D., Kerr, R.M., 2002. Transient vortex events in the initial value problem for turbulence. *Phys. Rev. Lett.* 88, 244501–
244505.
- 25 Kerr, R.M., 1985. Higher order derivative correlations and the alignment of small-scale structures in isotropic numerical
turbulence. *J. Fluid Mech.* 153, 31–58.
- 27 Kerr, R.M., 1992. Topological aspects of the dynamics of fluids and plasmas. In: Moffatt, H.K., Zaslavsky, G.M., Tabor, M.,
Comte, P. (Eds.), *Proceedings of the NATO-ARW Workshop at the Institute for Theoretical Physics, University of California*
at Santa Barbara. Kluwer, Dordrecht.
- 29 Kerr, R.M., 1993. Evidence for a singularity of the three-dimensional, incompressible Euler equations. *Phys. Fluids A* 5,
1725–1746.
- 31 Kerr, R.M., 1996. Cover illustration: vortex structure of Euler collapse. *Nonlinearity* 9, 271–272.
- 33 Kerr, R.M., 1999. The outer regions in singular Euler. In: Tsinober, Gyr (Eds.), *Fundamental Problematic Issues in Turbulence.*
Birkhäuser, Basel, pp. 41–48.
- 35 Kerr, R.M., Hussain, F., 1989. Simulation of vortex reconnection. *Physica D* 37, 474–484.
- Ohkitani, K., Gibbon, J.D., 2000. Numerical study of singularity formation in a class of Euler and Navier–Stokes flows. *Phys.*
Fluids 12, 3181–3194.
- Ohkitani, K., Yamada, M., 1997. Inviscid and inviscid-limit behavior of a surface quasi-geostrophic flow. *Phys. Fluids* 9,
876–882.
- Pumir, A., Siggia, E.D., 1987. Vortex dynamics and the existence of solutions of the Navier–Stokes equations. *Phys. Fluids* 30,
1606–1626.